Progress In Electromagnetics Research B, Vol. 75, 111–129, 2017

Low Noise Generation of RFI Noise Suppression Filter for Power Trace by Using Quarter-Wavelength Open-Stub Resonator in Multilayered High-Speed Digital PCB

Guang-Hwa Shiue*, Zhong-Yan You, Hao-Che Hung, and Shu-An Chou

Abstract—This work proposes a radio-frequency interference (RFI) noise suppression filter with low noise generation for a power trace. This is based on a quarter-wavelength open-stub resonator (QWOSR) in a multilayered high-speed digital PCB (printed circuit board). RFI noise with frequencies at 2.4 GHz and 5 GHz is considered. The proposed filter structure is a four-layer PCB. The low noise generation includes the following schemes. The trace of the QWOSR is a stripline on the third layer. Four ground vias are added adjacent to the QWOSR via, which is short. Electromagnetic (EM) radiation noise plan cavity resonance, ground bounce noise (GBN), and peak noise on insertion loss ($|S_{21}|$) are all reduced. The electric field distributions are elucidated to understand the effect of cavity resonance on the insertion loss ($|S_{21}|$) values of the proposed filter structure. The proposed filter structure significantly reduces the time-domain ground bounce and power noise whose frequency is equal or close to the center frequency of filter. Finally, favorable comparisons between simulated and measured results confirm the excellent low noise generation performance of the proposed filter structure.

1. INTRODUCTION

Wi-Fi is a technology for wireless local area networking, using devices that are based on the IEEE 802.11 standards [1]. Most modern consumer electronics have Wi-Fi technology for wireless communication. Wi-Fi typically uses 2.4 GHz and 5 GHz radio frequencies. In modern high-speed digital circuits in consumer electronics, high-speed time-varying switching currents on the power trace increase power noise. Since the bandwidth of a high-speed digital signal is very wide, the power noises can include radio frequency components (2.4 GHz and 5 GHz) [1], causing RFI of wireless circuits through antennas (Fig. 1) [2]. To prevent the generation of RFI noise, the radio frequency components of power noise on a power trace must be eliminated. Therefore, a bandstop filter is usually utilized to reduce RFI noise [3, 4]. Since Wi-Fi technology is generally used in modern consumer electronics, the rejection frequencies of the filter that is proposed herein are chosen 2.4 GHz and 5 GH.

Such transmission line stubs have been used before to enhance electromagnetic bandgap (EBG) structures [5, 6] and thereby to reduce the RFI noises on power/ground planes. An inexpensive and wideband common-mode noise suppression filter that uses a QWOSR has been comprehensively investigated [7]. Many bandstop filter designs that use microstrip coupled lines or quarter-wavelength open-stub resonators have been developed for many years [8]. In particular, a bandstop filter design that uses parallel coupled lines resonators has been proposed [9]; it utilizes electric or magnetic coupling between the transmission line and the QWOSR. The virtual ground fence (VGF) is proposed for filtering GHz power on PCBs [10]. The VGF is composed of transmission line stubs that are shorted to the power

Received 17 November 2016, Accepted 15 May 2017, Scheduled 27 May 2017

* Corresponding author: Guang-Hwa Shiue (ghs.apemclab@gmail.com).

The authors are with the Advanced Packaging and EMC Laboratory, Department of Electronic Engineering, The Chung Yuan Christian University, Taoyuan City, Taiwan 32023, R.O.C.

plane but routed on the ground plane. Since the transmission line stubs are located on the top layer (microstrip line structure) [8–10], large EM radiation (electromagnetic interference (EMI) problem) can occur.

This work proposes a new stopband filter structure that is based on the QWOSR to reduce RFI noise on a power trace of a high-speed digital circuit. The structure has four layers with two ground planes. The QWOSR trace is located on the third layer and connected by a via to the power trace. Four additional ground vias are connected between the two ground planes, adjacent to the QWOSR via. Therefore, the proposed filter can exhibit low GBN, power noise and EMI. Moreover, the proposed filter structure is very suitable for the use in modern multilayered high-speed digital PCBs.

The paper is organized as follows. Section 2 describes the problems of EM radiation loss and insertion loss ($|S_{21}|$) for different bandstop filters that include a QWOSR. Section 3 investigates the effects of parallel-plane resonance and GBN on the proposed filter. Section 4 presents some parameters analysis and noise reduction in the time domain. Section 5 compares simulated and measured results. Finally, Section 6 draws conclusions.

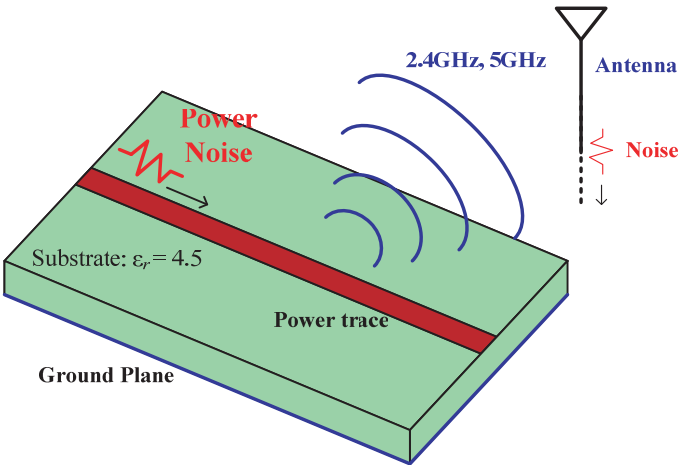

Figure 1. RFI by radio frequency components of power noise on power trace in wireless circuits through antenna.

2. STRUCTURE AND PROBLEM

Figures 2(a)–(d) schematically depict various bandstop filters that incorporate a QWOSR. Fig. 2(a) presents a conventional bandstop filter (structure a) [3]. The power trace and resonator trace in structure a (Fig. 2(a)) are both located on the top layer of the structure. The trace of the resonator in structure b (Fig. 2(b)) is under the power trace and connected to it by a via. Structure c is a three-layer stack with two ground planes. The trace of the resonator in structure c (Fig. 2(c)) is placed under the power trace in the second layer. The resonant trace in structure c is located on the ground plane (second layer) and isolated by a slot line as shown in Fig. 2(f) [9]. In this work, structure d (Fig. 2(d)) is the proposed filter structure which includes four additional ground vias that are joined to the QWOSR via. The structure is a four-layer structure with two ground planes. The QWOSR trace is located on the third layer and connected by a via to the power trace. Four additional ground vias are connected between two ground planes (layer two and layer four) (Fig. 2(f)). In structures c and d, these connections are at the four corners of the parallel ground planes, as shown in Figs. 2(g) and 2(h), respectively. Table 1 presents the geometric dimensions and materials of the four bandstop filters (structures a–d), as presented in Fig. 2.

A conventional QWOSR can be used in a narrow-band bandstop filter [3, 7, 11]. The desired rejection frequency, or resonant frequency, of the filter design determines the trace length (L) of the QWOSR. The equation for the length of the QWOSR [3] is

$$f_r \approx \frac{c}{4(L+L_v)\sqrt{\varepsilon_r}}(2n+1) \tag{1}$$

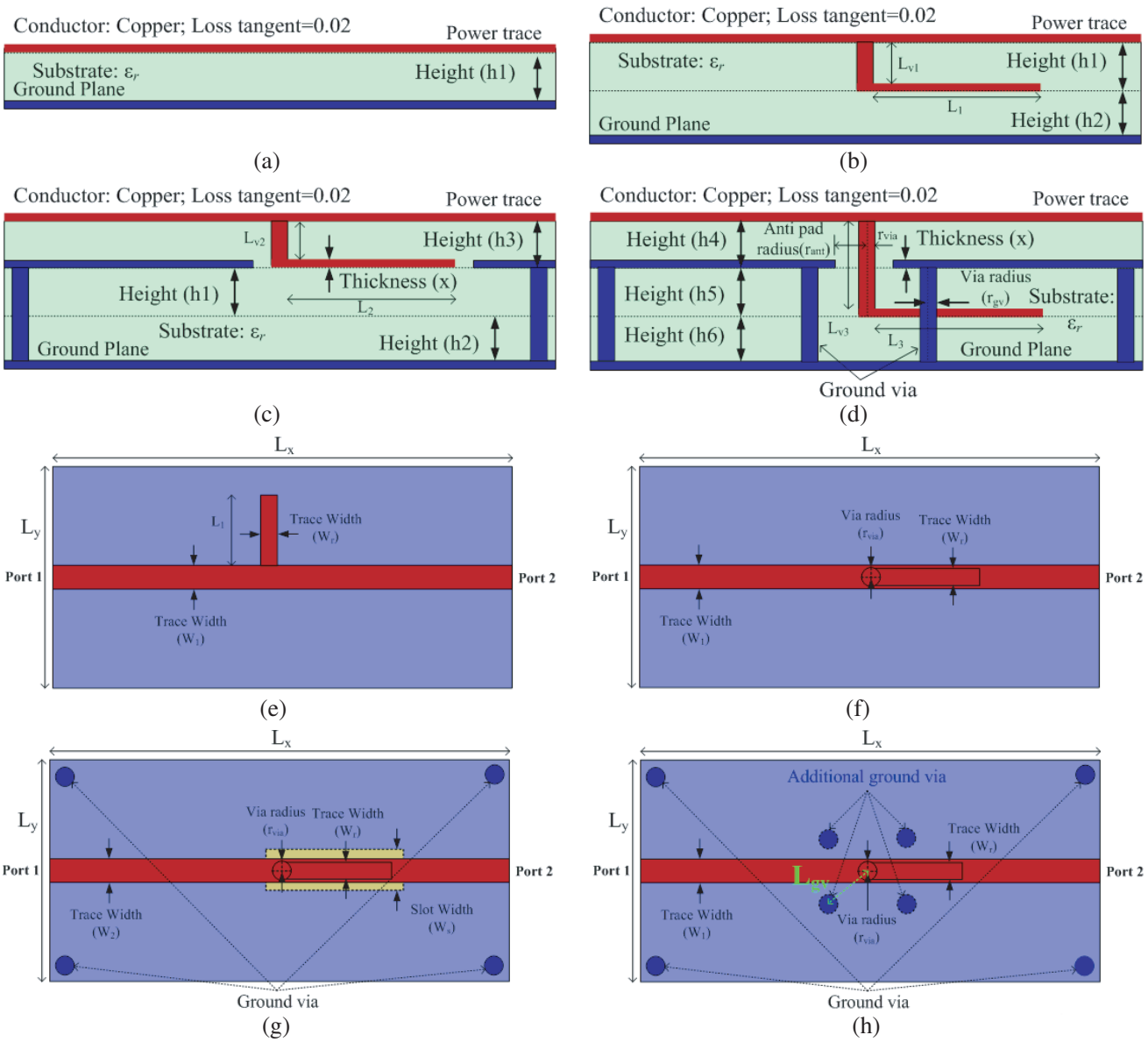

Figure 2. Side views of ((a) structure a, (b) structure b, (c) structure c, and (d) structure d) for a microstrip trace (power trace) with a QWOSR Top views of (e) structure a, (f) structure b, (g) structure c, (h) structure d.

where c is the speed of light in free space, ε_r the dielectric constant of the open stub, and n the resonance number ($n = 0, 1, 2, 3, \ldots$). The first resonant frequency is 2.4 GHz in Fig. 3(a) and 5 GHz in Fig. 3(b) in structures a–d. Owing to the 3-D nature of the all test structures, the 3-D full-wave simulator HFSS [12] is used to perform all frequency-domain simulations in this work.

Figure 3(c) shows 3 m radiation strength of the electric field ($|E_{3m}|$) in structures a–d for a power trace with a QWOSR with a resonant frequency of 2.4 GHz, and Fig. 3(d) shows the same structure with a resonant frequency of 5 GHz. According to Figs. 3(c) and 3(d), since the trace of QWOSR is located between two ground planes, structure d has the lowest $|E_{3m}|$ at a resonant frequency of 2.4 GHz or 5 GHz. Since in the three structures a–c the structure have a large $|E_{3m}|$, these structures cannot be used to reduce the RFI noise in high-speed digital circuits. Notably, the difference between $|E_{3m}|$ in the reference structure (structure a without a resonator) and that in structure d is slight. However, for structure d without four additional ground vias $|E_{3m}|$ is large for resonant frequencies of 2.4 GHz and

Table 1. Geometric dimensions and material properties of the various structures in Fig. 2.

W_1	W_2	W_r	W_s	h_1	h_2	h_3	h_4	h_5	h_6
18 mil	7 mil	40 mil	60 mil	9.4 mil	5.4 mil	4 mil	4 mil	11.4 mil	10 mil

x	r_{anti}	r_{via}	r_{gv}	Lx	Ly	L_{gv}	L_{v1}	L_{v2}	L_{v3}
1.4 mil	19 mil	8 mil	16 mil	1500 mil	600 mil	60 mil	4 mil	4 mil	15.4 mil

ε_r	L_s	L_1 (2.4 GHz)	L_2 (2.4 GHz)	L_3 (2.4 GHz)	L_1 (5 GHz)	L_2 (5 GHz)	L_3 (5 GHz)
4	331 mil	611 mil	611 mil	599.6 mil	291 mil	291 mil	279.6 mil

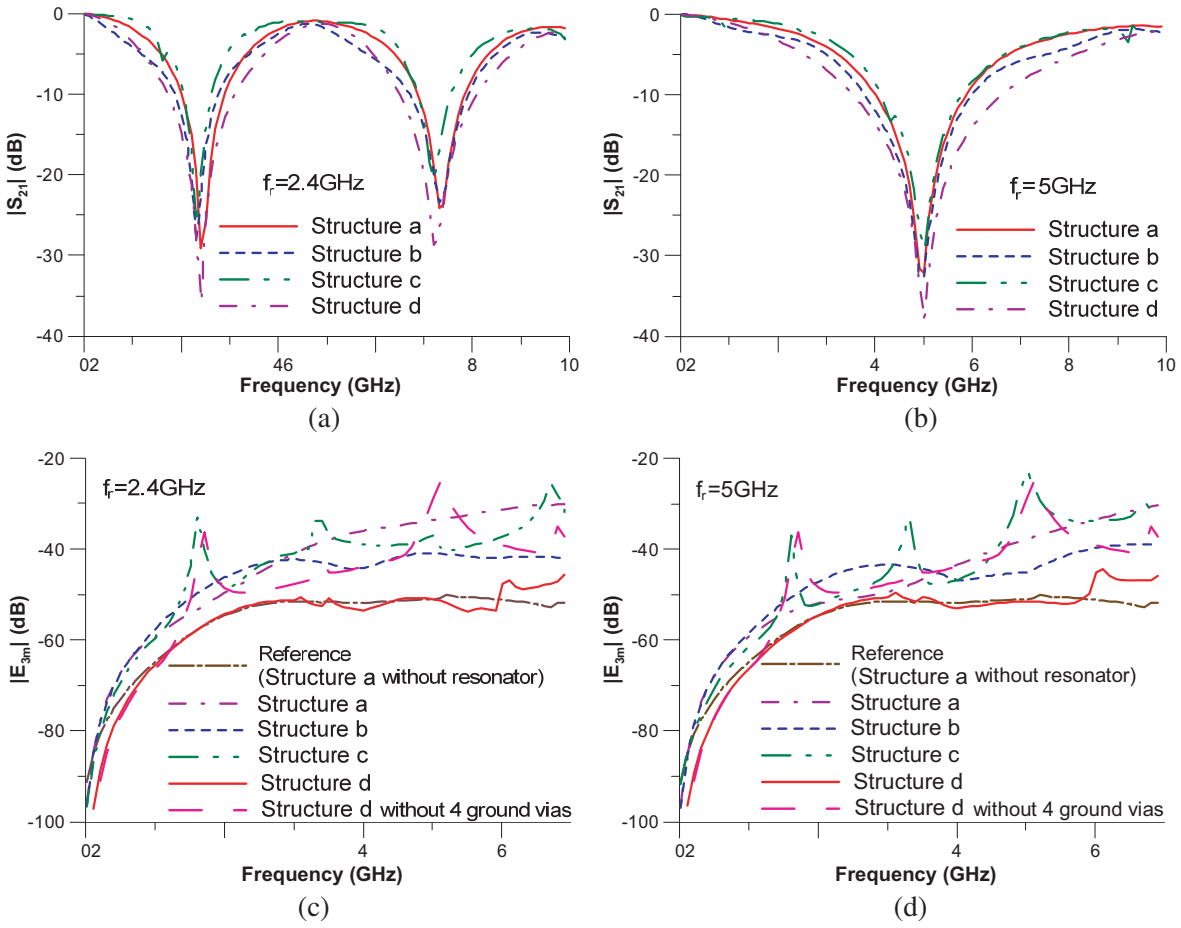

Figure 3. (a) Insertion loss ($|S_{21}|$) and (b) 3 m radiation strength of electric field in different structures (structure a, structure b, structure c, and structure d) of power trace with a QWOSR.

5 GHz, as shown in Figs. 3(c) and 3(d), respectively. Therefore, structure d requires the four additional ground vias to yield the lowest $|E_{3m}|$ at resonant frequencies of 2.4 GHz and 5 GHz.

Consequently the radio frequency components (2.4 GHz or 5 GHz) of the power noise on a high-speed digital power trace must be reduced, so this work proposes a power trace with an RFI noise suppression filter which comprises of QWOSR and four additional ground vias.

3. PLANE NOISE EFFECT

3.1. Parallel-Plane Resonant Effect on Inserted Loss

Cavity resonance is well known to occur in parallel metal plates [13]. Based on structure d in the previous section, three basic cases (case 1, case 2, and case 3) with/without four additional ground vias are provided to investigate the effect of this resonance on insertion loss. The main variation among the three cases is in the length of the QWOSR via. The longest and shortest vias are in cases 3 and 1, respectively. Table 2 presents the geometric dimensions of the three basic test structures. Fig. 4 shows side views of six test structures for a microstrip trace (power trace) with a QWOSR ((a-1) case 1 with four additional ground vias, (a-2) case 1 without four additional ground vias, (b-1) case 2 with

Table 2. Geometric dimensions of three basic test cases.

	h_5	h_6	L_1 (2.4 GHz)	L_2 (2.4 GHz)	L_1 (5 GHz)	L_2 (5 GHz)
Case 1	5.4 mil	15 mil	604.6 mil	10.4 mil	284.6 mil	10.4 mil
Case 2	11.4 mil	10 mil	599.6 mil	15.4 mil	279.6 mil	15.4 mil
Case 3	16.4 mil	5 mil	594.6 mil	20.4 mil	274.6 mil	20.4 mil

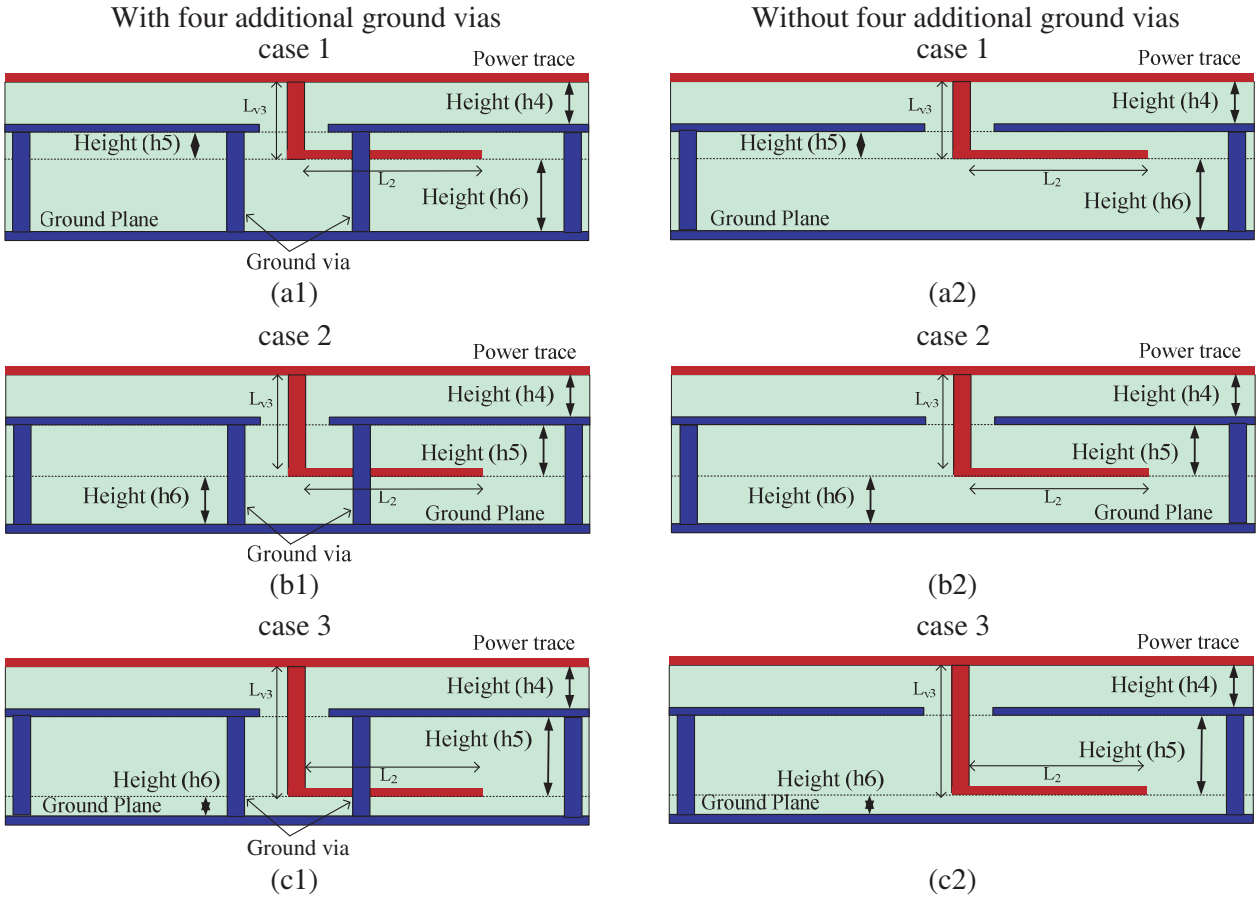

Figure 4. Side views of various proposed structures for obtaining a microstrip trace (power trace) with a QWOSR ((a-1) case 1 with four additional ground vias, (a-2) case 1 without four additional ground vias, (b-1) case 2 with four additional ground vias, (b-2) case 2 without four additional ground vias, (c-1) case 3 with four additional ground vias, and (c-2) case 3 without four additional ground vias).

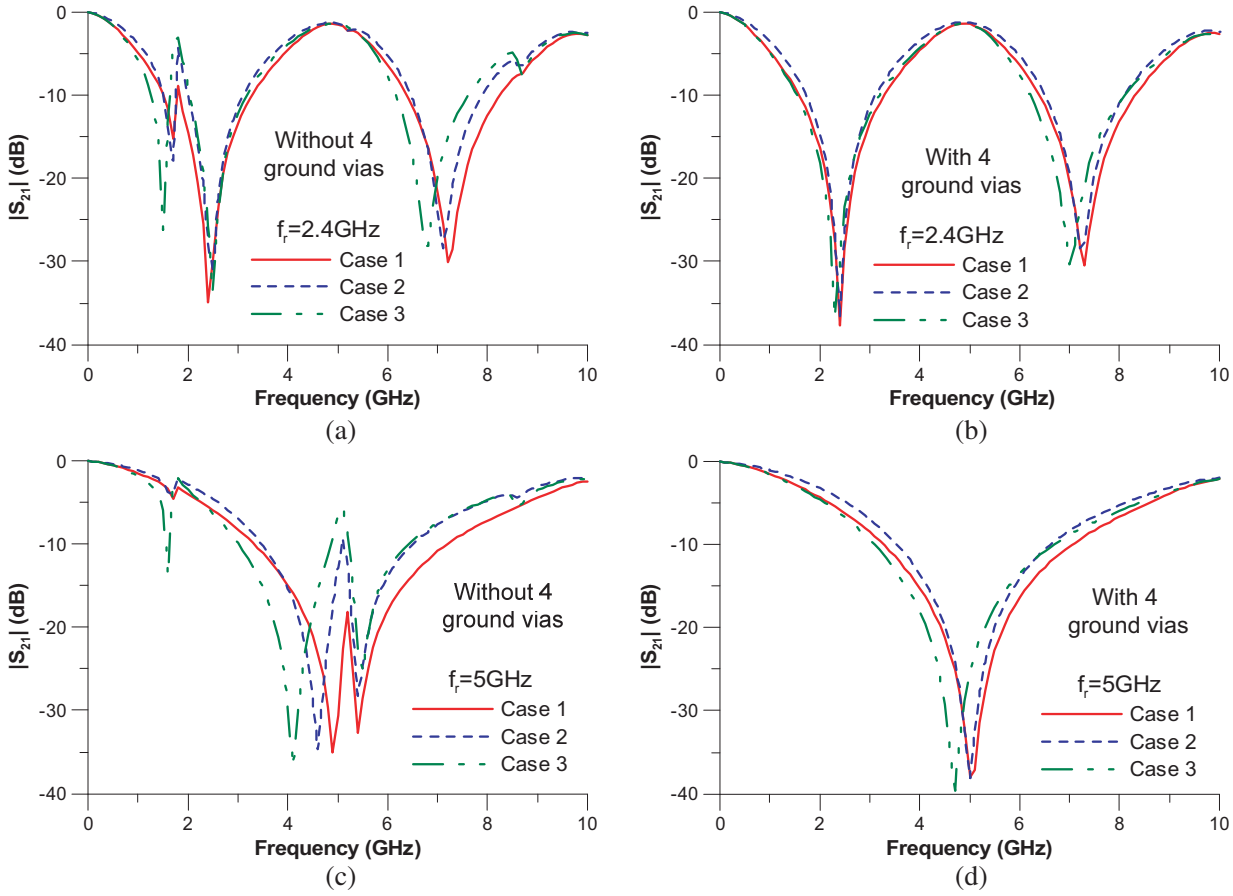

Figure 5. Comparisons of $|S_{21}|$ values obtained in simulations of power trace with QWOSR.

four additional ground vias, (b-2) case 2 without four additional ground vias, (c-1) case 3 with four additional ground vias, and (c-2) case 3 without four additional ground vias). The effect of the via length on QWOSR is also studied.

Figure 5 compares $|S_{21}|$ values obtained in simulations of a power trace with a QWOSR with/without four additional ground vias. The results are obtained with resonant frequencies of the QWOSR of 2.4 GHz and 5 GHz. Clearly, the $|S_{21}|$ values exhibit some peak responses, as shown in Figs. 5(a) and 5(c). However, the $|S_{21}|$ values in Figs. 5(b) and 5(d) exhibit almost no peak responses. The QWOSR via can excite the displacement current and propagate in the radius direction between the two ground planes in the absence of ground vias [14, 15]. The four additional ground vias are well known to help provide a current return path of displacement current excited by QWOSR via because the impedance of the ground via approaches $0\,\Omega$ (shorting path) [16, 17].

However, according to Figs. 6 and 7, the peak responses of the $|S_{21}|$ values are at resonant frequencies of the parallel planes that are coupled to power trace by the QWOSR via [18]. To investigate the relationship between the frequencies of the peak responses and the parallel-plane resonant frequencies, parallel-planes of three sizes, $L_y = 300$ mil, $L_y = 600$ mil, and $L_y = 900$ mil, are considered in case 2 without four additional ground vias (Fig. (a2)), and a resonant frequency of 5 GHz is utilized. Three identical parallel-plane structures with one excitation port at the position of the via of the QWOSR (Fig. 6(a)) are also compared.

Figure 6(a) shows $|S_{11}|$ of the three differently sized parallel-plane structures. Fig. 6(b) shows the $|S_{21}|$ of three differently sized proposed structures (case 2) without four additional ground vias. Owing to variation in size, the resonant frequencies on $|S_{11}|$ values and some peak responses on the $|S_{21}|$ values vary. Fig. 6(a) plots the $|S_{11}|$ values of the structure with four additional ground vias. In the case with four additional ground vias, the values of $|S_{11}|$ exhibit almost no resonance. Therefore,

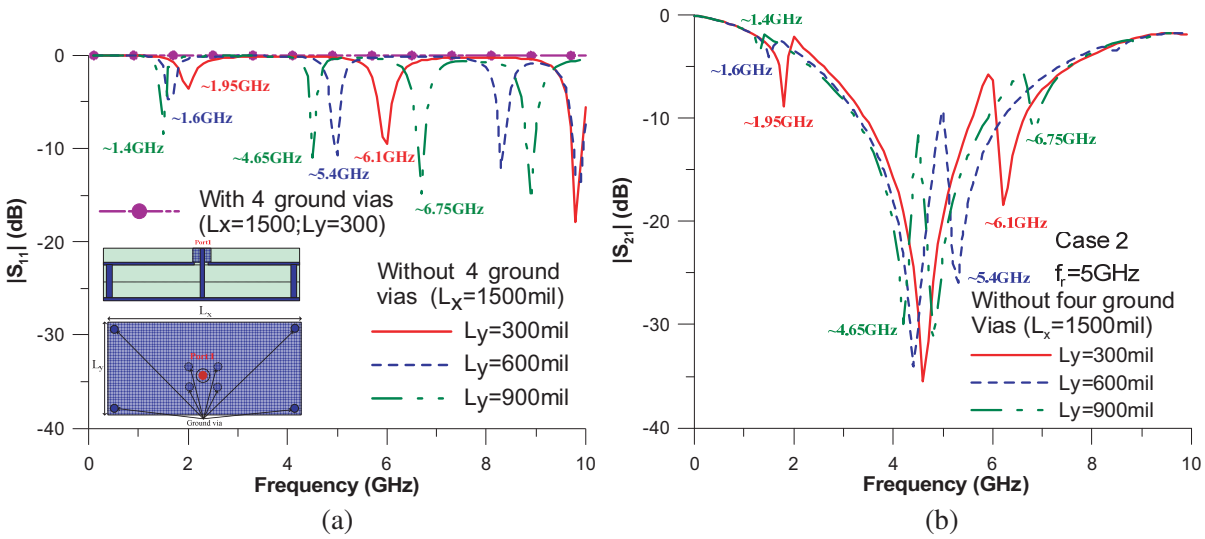

Figure 6. (a) Comparison of $|S_{11}|$ values obtained in simulations of parallel-plane structures with various plane sizes. (b) Comparison of $|S_{21}|$ values obtained in simulations of power trace with a QWOSR, without four additional ground vias (case 2), and with variously sized planes.

since the four additional ground vias can help provide a favorable current return path [17], the parallel-plane resonance is significantly degraded. Fig. 7 compares the electric field distributions of two ground planes on the electric field test plane in the two structures. Figs. 7(a1) and 7(a2) show almost equal resonant frequencies ((Figs. (b1) and (b2)) ~ 1.4 GHz, (Figs. (c1) and (c2)) ~ 1.6 GHz, (Figs. (d1) and (d2)) ~ 1.95 GHz, (Figs. (e1) and (e2)) ~ 4.65 GHz, (Figs. (f1) and (f2)) ~ 5.2 GHz, (Figs. (g1) and (g2)) ~ 6.1 GHz, and (Figs. (h1) and (h2)) ~ 6.75 GHz.). Clearly, the electric field distributions of the resonant frequencies of the structure (Fig. 7(a1)) are the same as those associated with the peak responses on the $|S_{21}|$ values of the structure (Fig. 7(a2)). Accordingly, some peak responses of $|S_{21}|$ values of the proposed filter structure without four additional ground vias are coupled from the parallel-plane resonance by the QWOSR via. Additionally, according to Figs. 7(a1)–7(h3), filter structures without four additional ground vias can excite large parallel-plane resonance between the two ground planes (Figs. 7(a1)–7(h1) and 7(a2)–7(h2)), and those with four additional ground vias can excite very small parallel-plane resonance between the two ground planes (Figs. 7(a3)–7(h3)).

In Figs. 5(a) and 5(c), since the long via of the QWOSR can be excited and a larger parallel-plane resonance can be induced [18], the peak response of $|S_{21}|$ values is large. Therefore, according to Figs. 5(b) and 5(d), the response of the $|S_{21}|$ values in case 1 (with the shortest via of the QWOSR) is the best. Consequently, the proposed filter structure with shorter vias of the QWOSR (case 1) is proposed.

3.2. Ground Bounce Effect

GBN is of increasing concern in high-speed digital circuits as data rates increase and voltages fall. This noise can cause false switching in digital circuits and breakdown in analog circuits. Largely owing to high-speed time-varying currents through the vias in the parallel-plate layer, this noise may cause significant signal integrity problems and electromagnetic interference (EMI) in high-speed digital circuits [18, 19]. Based on the results in the preceding section concerning the proposed filter structure without four ground vias, cavity resonance occurs in the parallel metal plane structure. The plane resonance can cause GBN.

To investigate the effect of GBN on the proposed filter structure, a ramped step source with an amplitude 2 V and t_r of 50 ps is input into port 1 of the proposed filter structure, as shown in Fig. 8(a). Fig. 8(a) presents the test point x of GBN (V_{gb}) between two ground planes. This section compares the related results for the three test structures which are the same as the three structures (1, 2, and

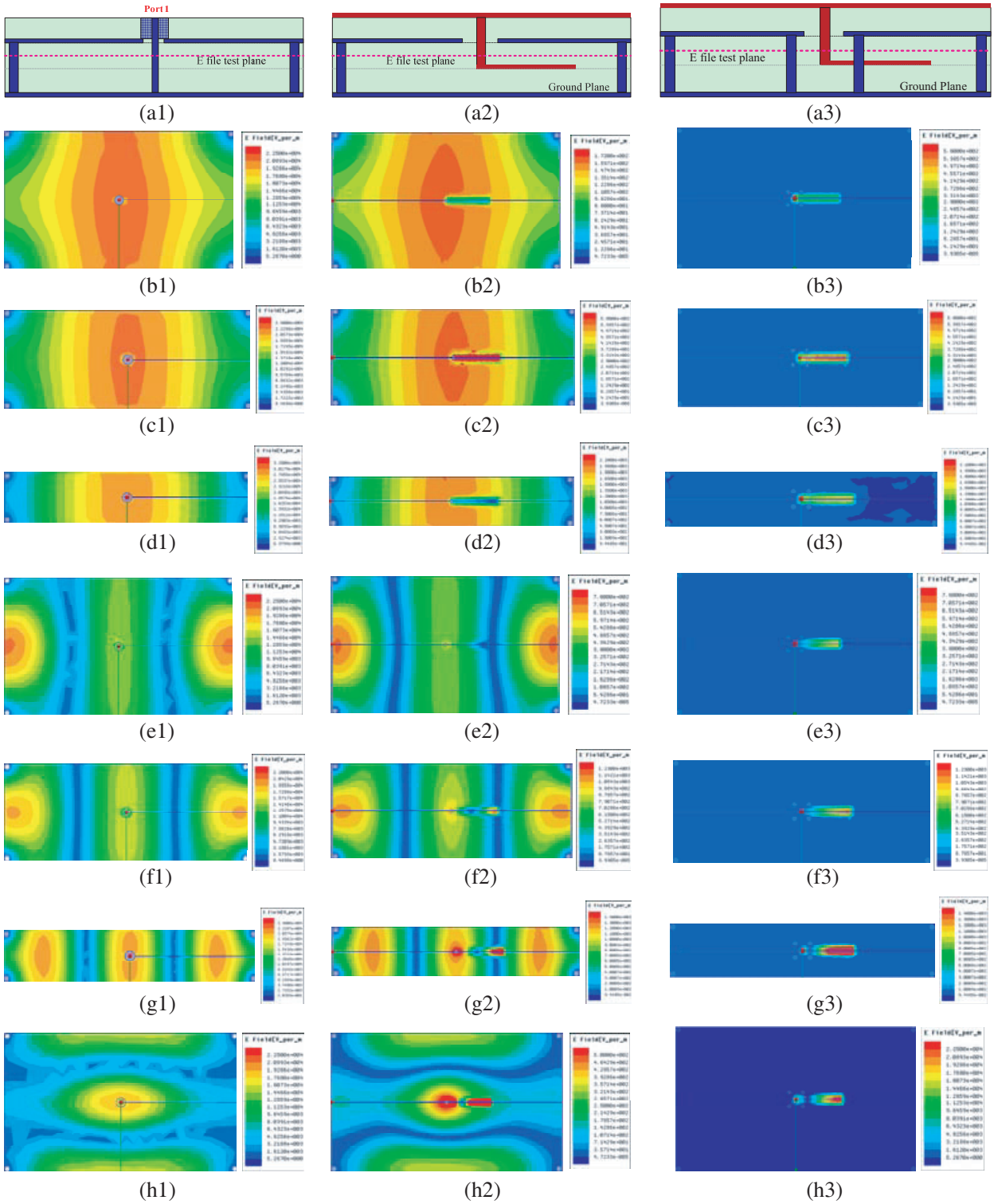

Figure 7. Comparisons of electric field distributions between two ground planes on the electric field test plane in three structures ((a1), (a2) and (a3)) with almost equal resonant frequencies ((b1) (b2) (b3) $\sim$ 1.4 GHz, (c1) (c2) (c3) $\sim$ 1.6 GHz, (d1) (d2) (d3) $\sim$ 1.95 GHz, (e1) (e2) (e3) $\sim$ 4.65 GHz, (f1) (f2) (f3) $\sim$ 5.2 GHz, (g1) (g2) (g3) $\sim$ 6.1 GHz, and (h1) (h2) (h3) $\sim$ 6.75 GHz.

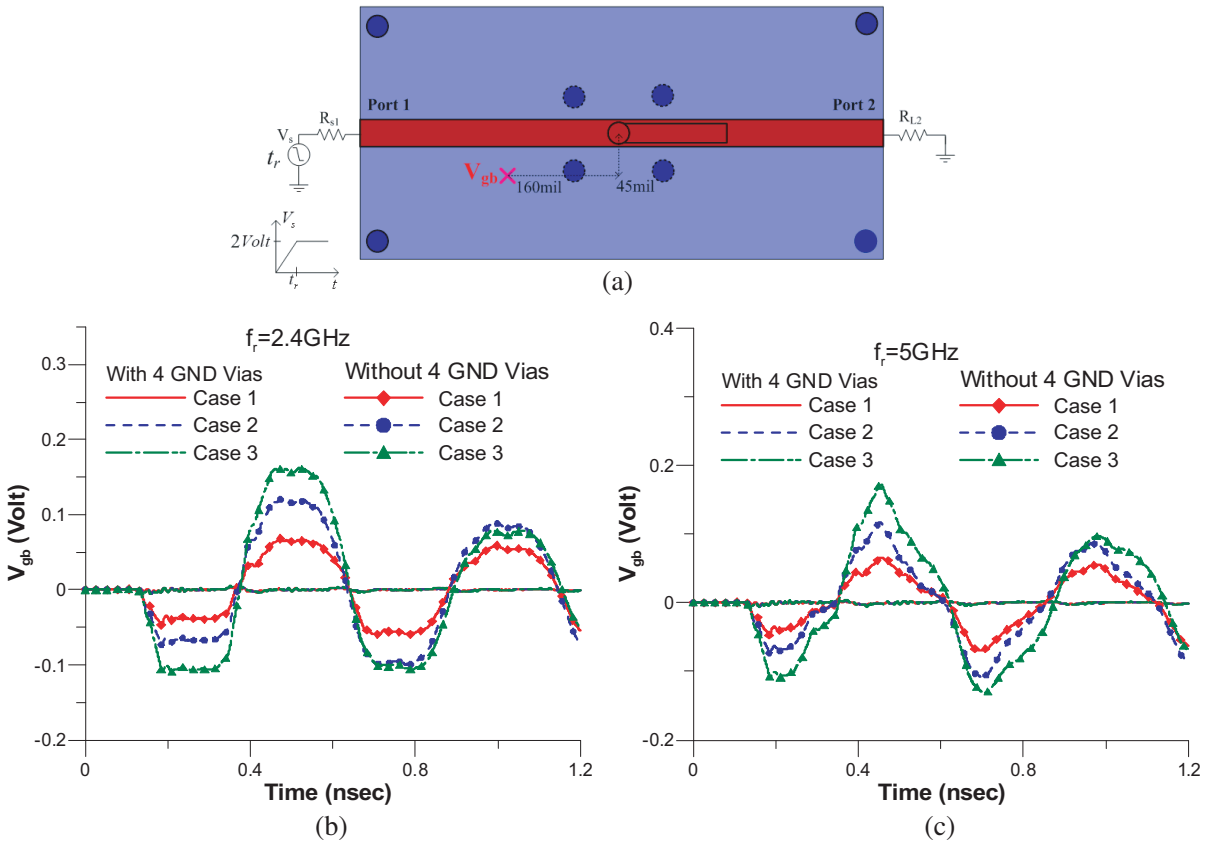

Figure 8. Comparisons of simulated time-domain GBN (V_{gb}) of three cases (1, 2, and 3) with/without four additional ground vias at resonant frequencies of 2.4 GHz and 5 GHz.

3) in Fig. 4. Figs. 8(b) and 8(c) compare the simulated time-domain GBN V_{gb} in the three cases with/without four additional ground vias at resonant frequencies of 2.4 GHz and 5 GHz. Clearly, for a structure without four additional ground vias, a long via of the QWOSR results in a large GBN. For the structures with four additional ground vias, the GBN is very small with a resonant frequency of 2.4 GHz (Fig. 8(b)) or 5 GHz (Fig. 8(c)).

GBN exists in the proposed parallel metal planes filter structure without four additional ground vias. Coupled noise (V_{cn}) can be induced at port 3 (Fig. 9(a)) by the slot line through GBN [20]. The length (S_l) and width (W_{s2}) of the slot line are 383.7 mm and 19 mm, respectively. The distances S_x and S_y are set to 120 mm and 140 mm, respectively. The trace width (W_3) and length (T_l) of the trace on layer one are 7 mm and 200 mm, respectively. Figs. 9(a) and 9(b) compare the three structures (cases 1, 2, and 3) with a slot line, with/without four additional ground vias, at resonant frequencies of 2.4 GHz and 5 GHz in terms of the simulated coupled noise (V_{cn}). Clearly, for the structure without four additional ground vias, the long via of the QWOSR results in large coupled noise. Furthermore, for structures with four additional ground vias, the coupled noise is small at a resonant frequency of 2.4 GHz or 5 GHz. Therefore, a large coupled noise indicates a large GBN [2]. Therefore, for convenience, in the following section, the structure in Fig. 9(a) is adopted to confirm the GBN reduction achieved using four additional ground vias.

4. MORE INVESTIGATIONS

According to the results in the previous section, a short via of a QWOSR (case 1) can yield a small GBN and favorable insertion loss $|S_{21}|$. Therefore, case 1 (with the shortest via of the QWOSR) is adopted below.

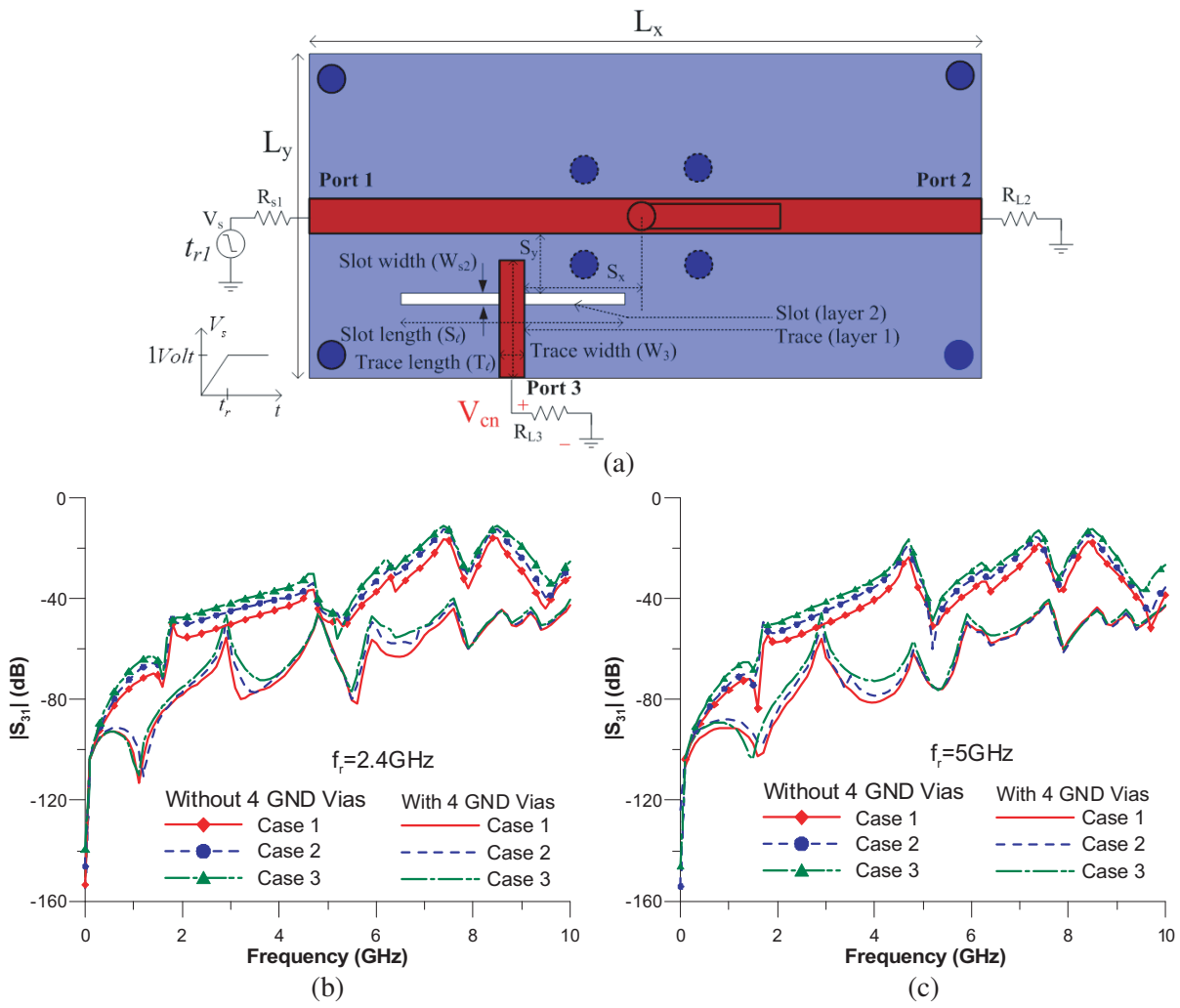

Figure 9. Comparisons of simulated coupled noise (V_{cn}) of) three cases (1, 2, and 3) with a slot line, with/without four additional ground vias, at resonant frequencies of (a) 2.4 GHz and (b) 5 GHz.

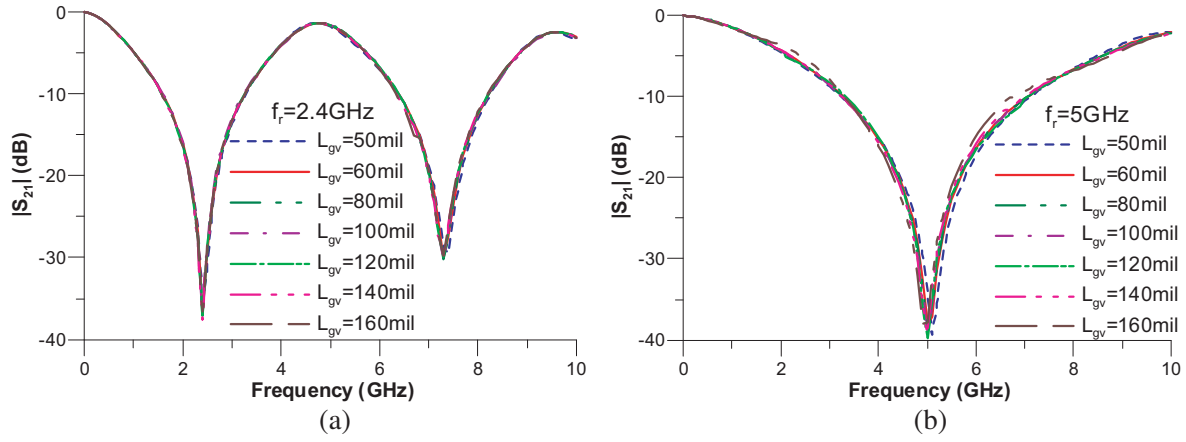

Figure 10. Comparisons of $|S_{21}|$ values obtained in simulations of proposed filter structure with various L_{gv} for (a) $f_r = 2.4$ GHz and (b) $f_r = 5$ GHz.

4.1. Some Parameters Analysis and Design Guidelines

Figure 10 compares the $|S_{21}|$ values obtained in simulations of the proposed filter structure with various distances (L_{gv}) between additional ground vias and the QWOSR via for $f_r = 2.4\,\text{GHz}$ and $f_r = 5\,\text{GHz}$. From Fig. 10, the variations of $|S_{21}|$ values are very small at $f_r = 2.4\,\text{GHz}$ and small at $f_r = 5\,\text{GHz}$. However, in Fig. 10(b), for small L_{gv} the resonant frequency is shifted toward high frequency. However, the shift is still very small. Additionally, Fig. 11 compares the values of the time-domain V_{gb} and frequency-domain V_{cn} obtained in simulations of the proposed filter structures with various L_{gv} for $f_r = 2.4\,\text{GHz}$ and $f_r = 5\,\text{GHz}$. The simulated structure and time-domain GBN (V_{gb}) are the same as in Fig. 8(a). The simulated structure and frequency-domain coupled noise (V_{gb}) are as in Fig. 9(a). However, the distances S_x and S_y are 120 mm and 140 mm, respectively. Clearly, from Fig. 11, a large distance L_{gv} can generate a large GBN not only in the time domain, but also in the frequency domain. However, a large distance (L_{gv}) with large GBN can be obviously found after 5 GHz in $|S_{21}|$ values. For $f_r = 2.4\,\text{GHz}$ (Figs. 11(a) and 11(b)) and $f_r = 5\,\text{GHz}$ (Figs. 11(c) and 11(d)), the same results are obtained.

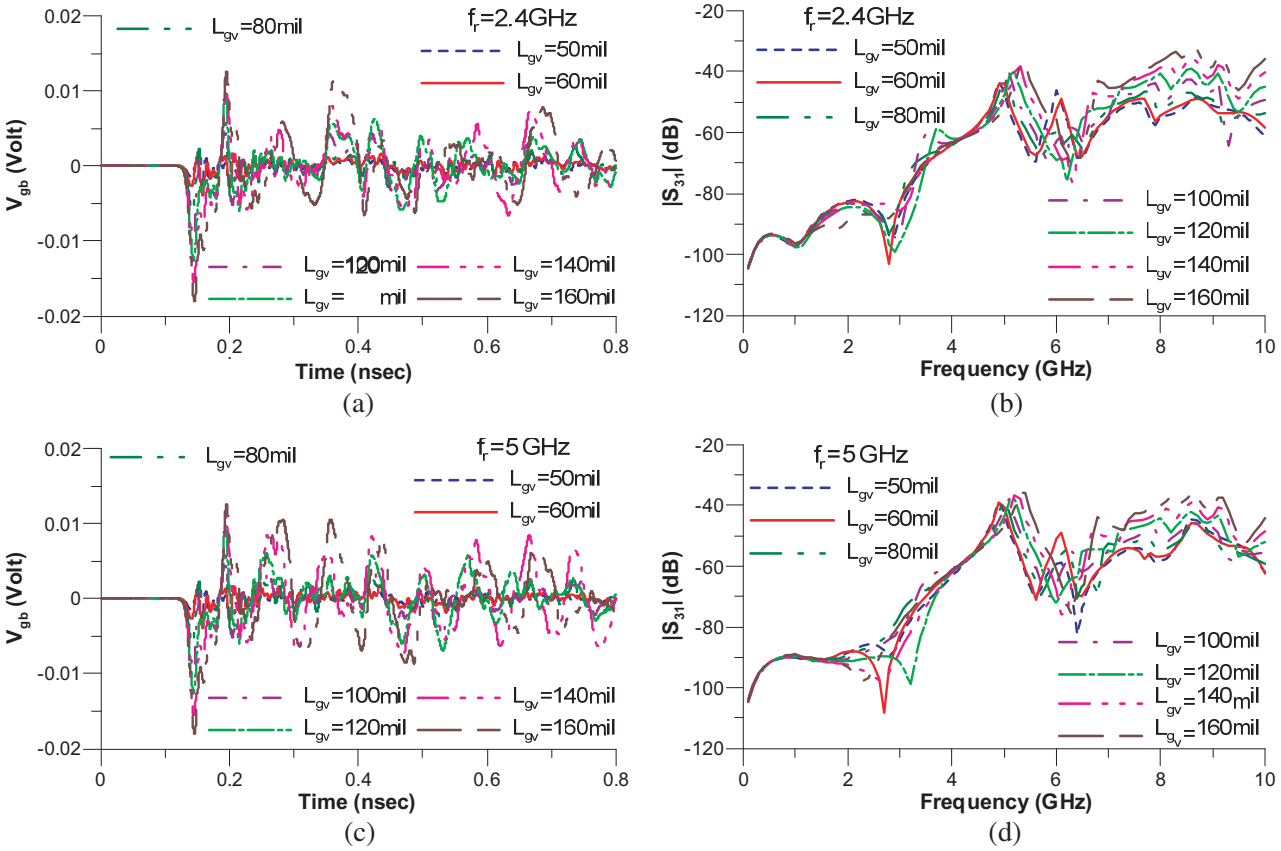

Figure 11. Comparisons of time-domain V_{gb} and frequency-domain V_{cn} obtained in simulations of proposed filter structure with various L_{gv} for (a) (b) $f_r = 2.4\,\text{GHz}$ and (c) (d) $f_r = 5\,\text{GHz}$.

Figure 12 compares the $|S_{21}|$ values obtained in simulations of the proposed filter structure with various r_{gv} (radius of ground vias) for $f_r = 2.4\,\text{GHz}$ and $f_r = 5\,\text{GHz}$. The radius of the ground vias almost does not affect $|S_{21}|$. Fig. 13 compares the $|S_{21}|$ values obtained in simulations of the proposed filter structure with various values of W_r (trace width of QWOSR) for $f_r = 2.4\,\text{GHz}$ and $f_r = 5\,\text{GHz}$. Clearly, a wider trace results in a larger bandwidth. Fig. 14 compares the $|S_{21}|$ values obtained in simulations of the proposed filter structure with various values of r_{via} (radius of via of QWOSR) for $f_r = 2.4\,\text{GHz}$ and $f_r = 5\,\text{GHz}$. Obviously, a larger radius results in a higher resonant frequency. The

variations in $|S_{21}|$ is very small at $f_r = 2.4\,\text{GHz}$ and small at $f_r = 5\,\text{GHz}$. However, in Fig. 10(b), as r_{via} increases the resonant frequency increases. Fig. 15 compares the $|S_{21}|$ values obtained in simulations of the proposed filter structure with different values of r_{via} (antipad of via of QWOSR) for $f_r = 2.4\,\text{GHz}$ and $f_r = 5\,\text{GHz}$. Clearly, a larger antipad results in a higher resonant frequency. However, the shift is very small.

Based on the results in Figs. 8–15, the following guidelines for the design of the proposed filter structure are proposed. The values of the related geometric dimensions refer to Figs. 8–15. Additionally, the PCB stackup consists of at least four layers (Fig. 2(d)).

(1). Choose the minimum length (L_{via}) of the QWOSR via. (Figs. 8 and 9).

(2). Choose the minimum distance (L_{gv}) between QWOSR via and additional ground via. (Fig. 11).

(3). Choose the larger width (W_r) of the QWOSR trace. (Fig. 13).

(4). Choose the smaller radius (r_{via}) and antipad (r_{anti}) of the QWOSR via. (Figs. 14 and 15).

(5). Choose a radius (r_{gv}) of the additional ground via in the range: 6 mil–16 mil. (Fig. 12).

(6). Based on the desired suppressing frequency, use formula (1) to determine the length of the QWOSR trace.

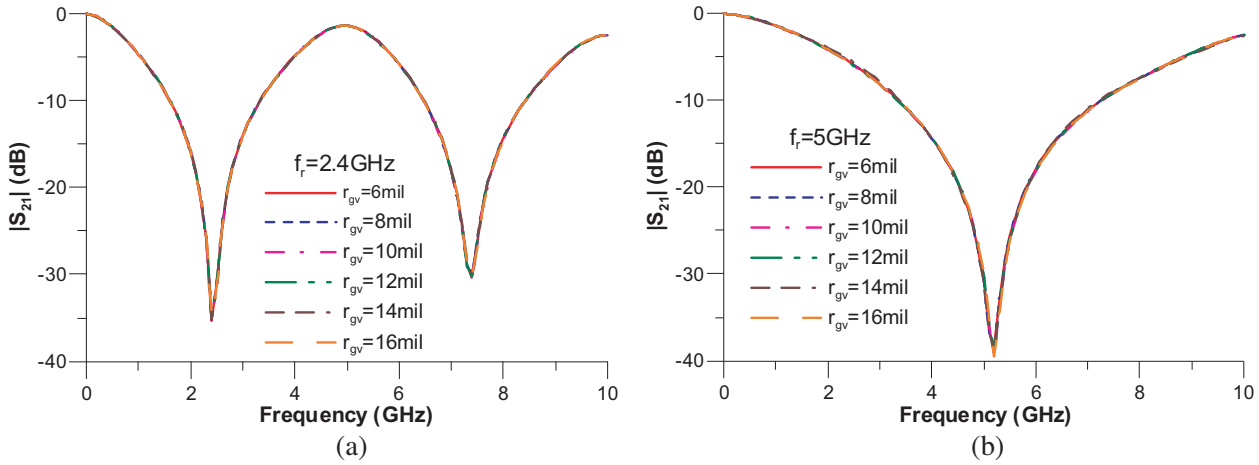

Figure 12. Comparison of $|S_{21}|$ values obtained in simulations of proposed filter structure with different r_{gv} for (a) $f_r = 2.4\,\text{GHz}$ and (b) $f_r = 5\,\text{GHz}$.

4.2. Time-Domain Noise Reduction

To investigate the performance of time-domain noise (power noise) reduction, Fig. 16 shows the top view of the proposed filter structure. Since the noise source is connected to port 1, the QWOSR is also placed near port 1, as shown in Fig. 16(a). For simplicity, the noise source is a sinusoid wave with a peak-to-peak amplitude of 2 V. The initial voltage at port 1 of the power trace is 1 V. The frequencies of the noise source are set to 2.4 GHz/5 GHz for $f_r = 2.4\,\text{GHz}$ and 1 GHz/5 GHz for $f_r = 5\,\text{GHz}$ case, respectively. Figs. 16(b)–(e) compare the time-domain results (V_{tdt}) of the proposed filter structure with the noise source (V_{ns}) for $f_r = 2.4\,\text{GHz}$ and $f_r = 5\,\text{GHz}$.

Clearly, the amplitudes of the noise sources at that resonant frequency of QWOSR at port 2 (V_{tdt}) are both significantly degraded, as shown in Figs. 16(b) and 16(d). The $|S_{21}|$ values (Figs. 5(b) and 5(d)) of the proposed filter structure can be used to verify the results. Therefore, the amplitudes of the noise source at non-resonant frequencies (5 GHz/1 GHz) of the QWOSR at port 2 (V_{tdt}) are both slightly degraded, as shown in Figs. 16(c) and 16(d). Therefore, the proposed filter structure can significantly reduce power noise whose frequency is the same as or close to the resonant frequency (2.4 GHz and 5 GHz) of the QWOSR in the power trace, as shown in Figs. 16(b) and 16(e). The related following section on measurement validation will investigate the EM radiation reduction.

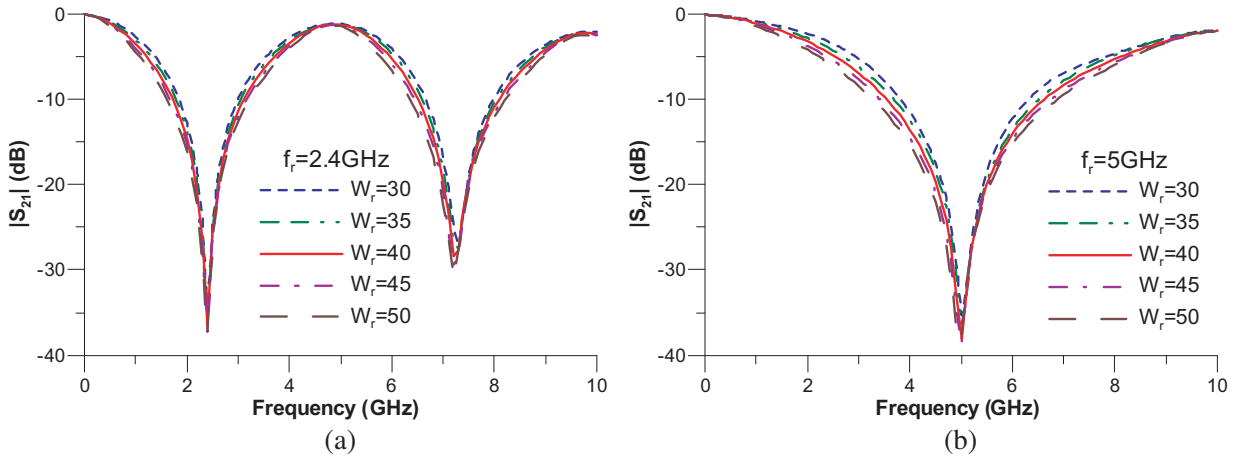

Figure 13. Comparisons of $|S_{21}|$ values obtained in simulations of proposed filter structure with different W_r for (a) $f_r = 2.4\,\text{GHz}$ and (b) $f_r = 5\,\text{GHz}$.

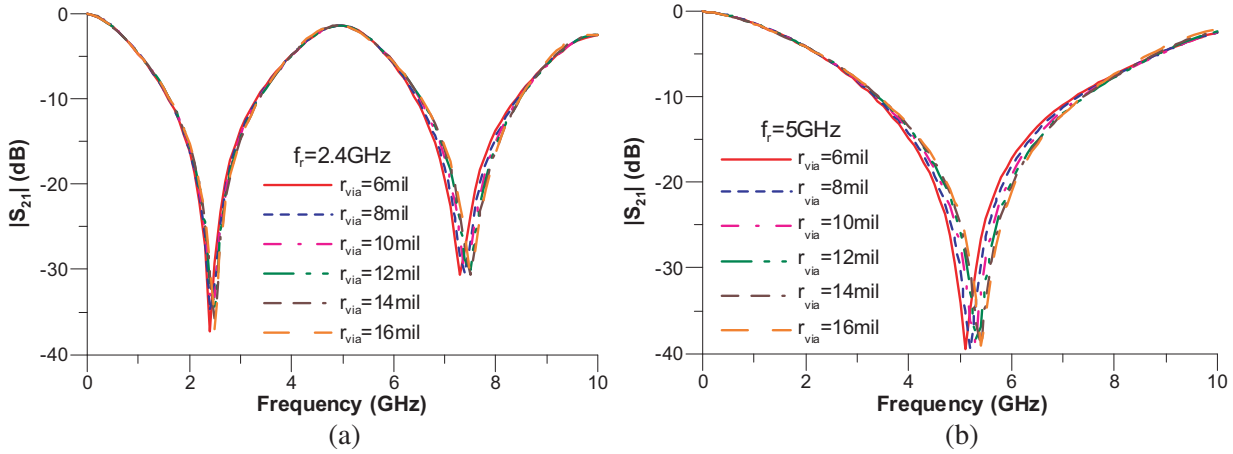

Figure 14. Comparisons of $|S_{21}|$ values obtained in simulations of proposed filter structure with different values of r_{via} for (a) $f_r = 2.4\,\text{GHz}$ and (b) $f_r = 5\,\text{GHz}$.

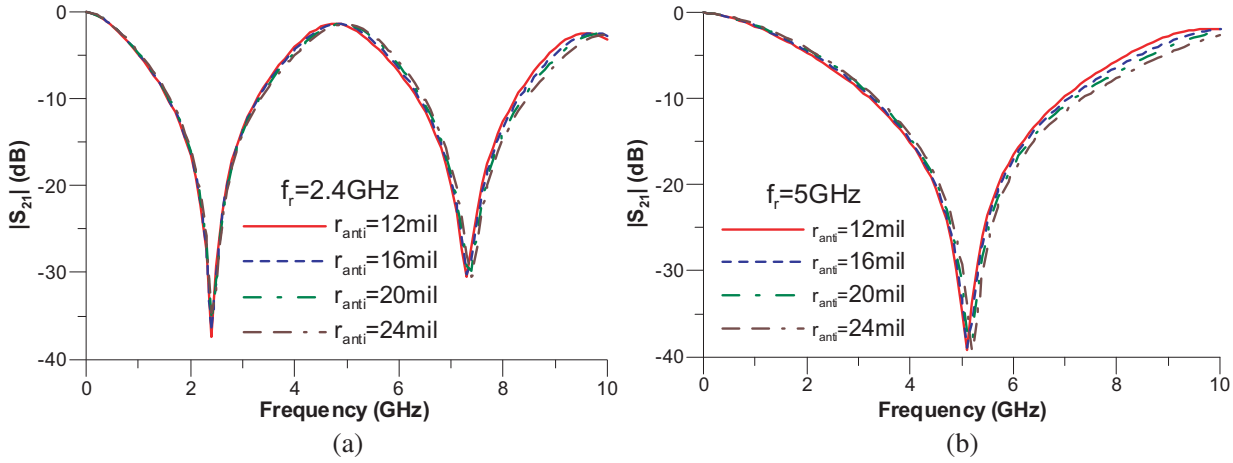

Figure 15. Comparisons of $|S_{21}|$ values obtained in simulations of proposed filter structure with different values of r_{anti} for (a) $f_r = 2.4\,\text{GHz}$ and (b) $f_r = 5\,\text{GHz}$.

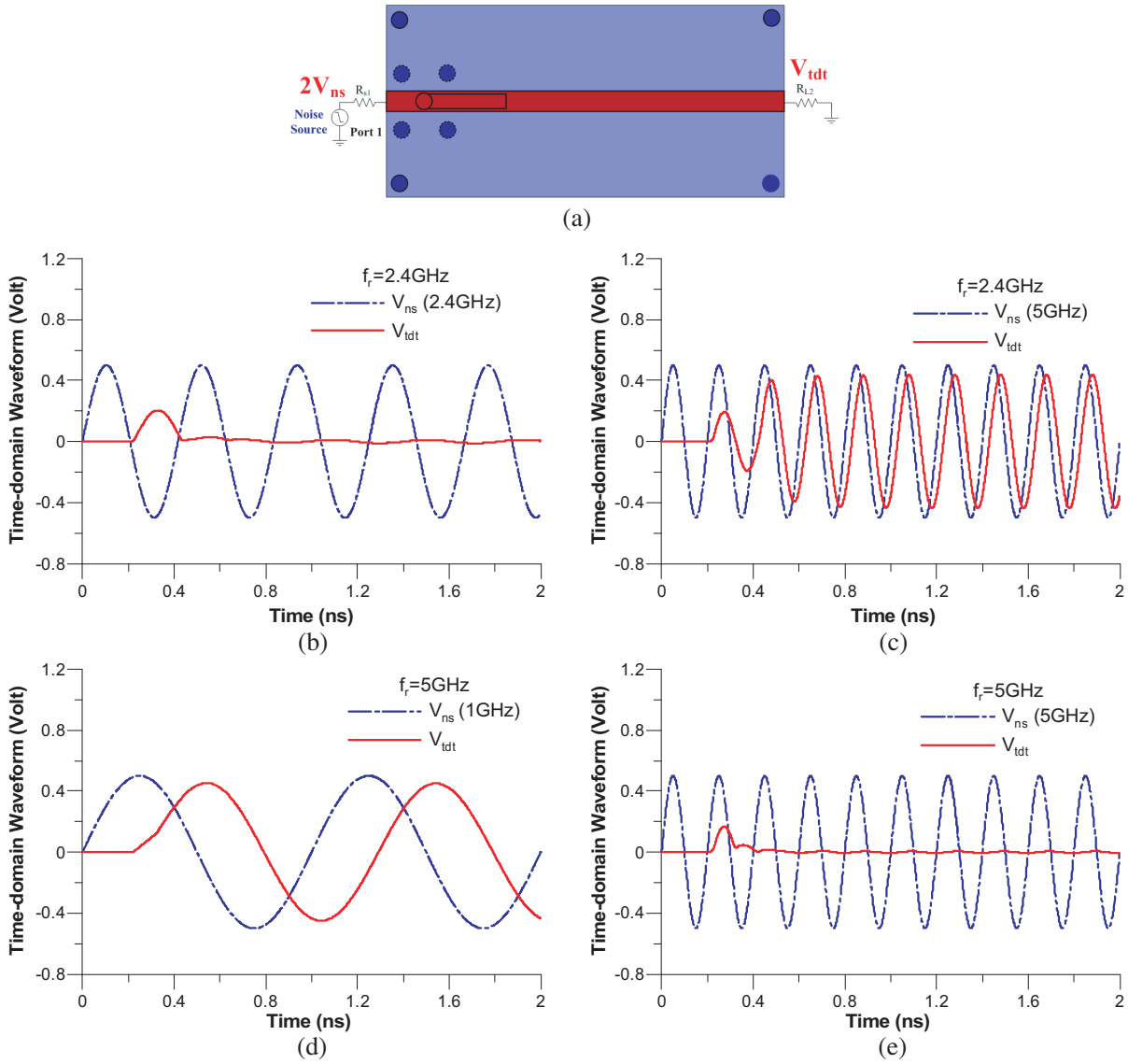

Figure 16. (a) Top view of proposed filter structure (with a QWOSR on the left side). (b)–(e) Comparisons of time-domain results (V_{tdt}) for proposed filter structure with noise source (V_{ns}) for $f_r = 2.4\,\text{GHz}$ and $f_r = 5\,\text{GHz}$.

5. MEASUREMENT VALIDATION

To verify low noise generation by the proposed filter structure (power trace with a QWOSR and four additional ground vias), simulated and measured results in the frequency domain are compared. Measurements are obtained for twelve measured boards (MBs): (1) MB 1 (Fig. 17(a)): the proposed filter structure without four additional ground vias (a power trace with only a QWOSR), (2) MB 2 (Fig. 17(b)): the proposed filter structure, (3) MB 3 (Fig. 17(c)): MB 1 with a tracecrossing slot line, (4) MB 4 (Fig. 17(d)): MB 2 with a tracecrossing slot line (5) MB 5 (Fig. 17(e)): MB 2 without QWOSR, and (6) MB 6 (Fig. 17(f)): the proposed filter structure (The QWOSR is placed close to port 1) (7) MB 7 (Fig. 17(g)): the proposed filter structure without four additional ground vias (a power trace with only a QWOSR), (8) MB 8 (Fig. 17(h)): the proposed filter structure, (9) MB 9 (Fig. 17(i)): MB 1 with a trace-crossing slot line, (10) MB 10 (Fig. 16(j)): MB 2 with a trace-crossing slot line, (11) MB 11 (Fig. 17(k)): MB 2 without QWOSR, and (12) MB 12 (Fig. 17(l)): the proposed

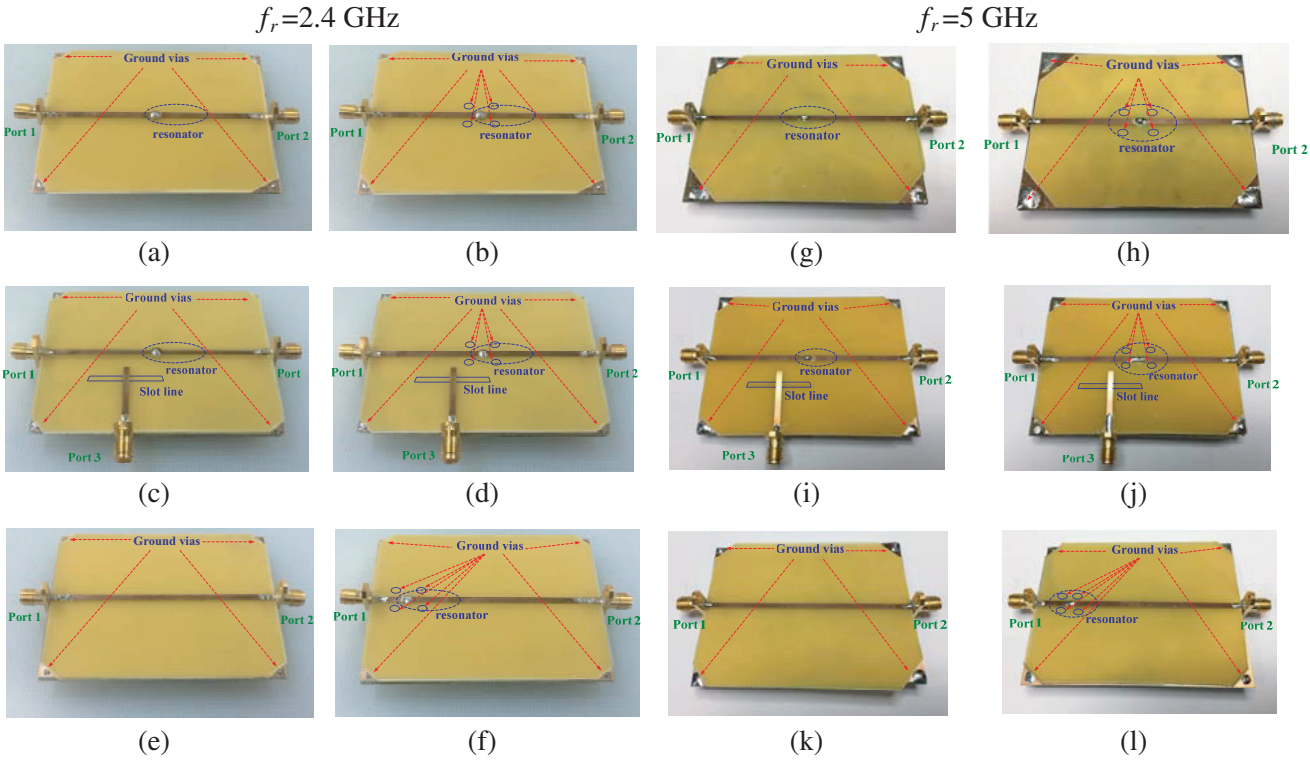

Figure 17. Photographs of 12 measured boards. ((a) MB 1, (b) MB 2, (c) MB 3, (d) MB 4, (e) MB 5, (f) MB 6, (g) MB 7, (h) MB 8, (i) MB 9, (j) MB 10, (k) MB 11, and (l) MB 12)).

Table 3. Dimensions and material parameters of measured boards.

W_1	W_2	W_r	W_s	h_1	h_2	h_3	S_ℓ	T_ℓ
2.25 mm	2.25 mm	0.85 mm	1.5 mm	1.2 mm	0.6 mm	1 mm	25 mm	24 mm
80 mm	60 mm	4.3 mm	1.835 mm	12.4 mm (2.4 GHz) 5.7 mm (5 GHz)	0.5 mm	0.5 mm	0.035 mm	4.4 mm

filter structure (with the QWOSR placed close to port 1). The laboratory implementation is simplified using boards fabricated on millimeter scale. The resonant frequency of measured boards MB 1–6 is set to 2.4 GHz and that of MB 7–12 set to 5 GHz. Table 3 presents the dimensions and material parameters of the measured boards. Fig. 17 shows photographs of all of the manufactured and measured boards.

The measured structures are simulated in the frequency domain using the 3-D full-wave simulator HFSS. Measurements using an Agilent/E5071B frequency-domain network analyzer are compared with the HFSS simulation results.

Figures 18 and 19 show the simulated and measured $|S_{21}|$ and $|S_{31}|$ for the proposed filter structure with/without four additional ground vias. The simulated results agree closely with the measurements. The deviations between the simulations and measurements are attributable to the neglecting of the SMA connectors in the simulations, small variations of the material properties of the substrate, small variations in the manufacturing process, the definition of the port(s), and other causes. This investigation also studies the suppression of the radiation of RFI noise in the power trace. The measurements are made using a vector network analyzer Agilent/E5071B. Fig. 20(a) shows the measurement setup. Since the port 1 signal excited by VNA is directly launched onto the power trace, the signal is regarded as power noise. The power noise passes through the power trace with and without

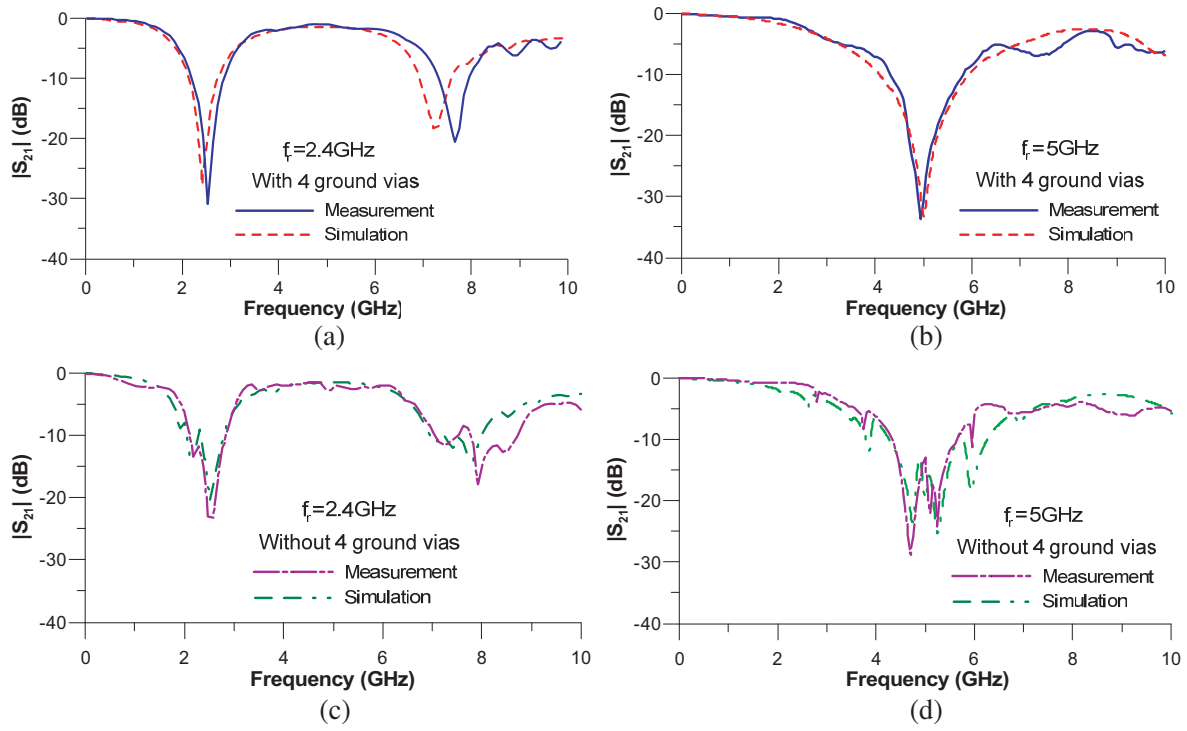

Figure 18. Comparisons of simulated and measured $|S_{21}|$ values of proposed filter structure (a) (b) with and (c) (d) without four additional ground vias.

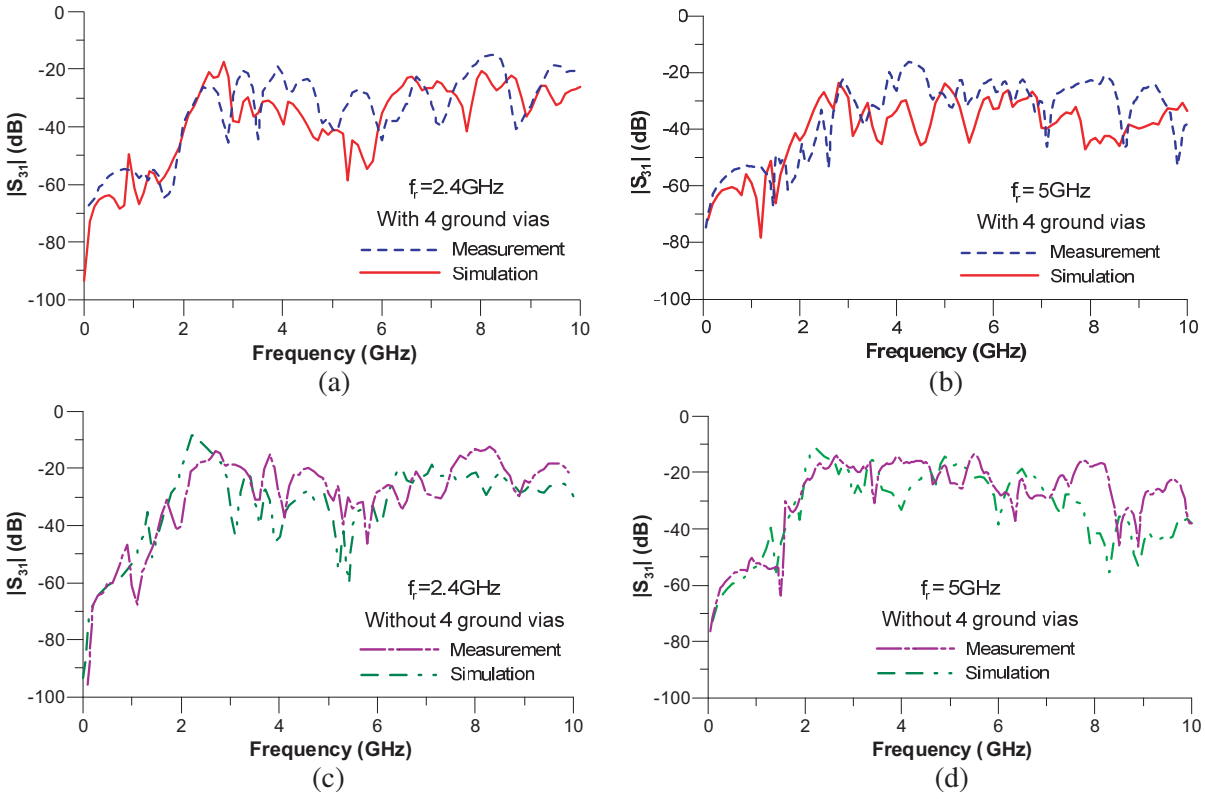

Figure 19. Comparisons of simulated and measured $|S_{31}|$ values (coupled noise) of proposed filter structure (a) (b) with and (c) (d) without four additional ground vias.

the QWOSR. The port 2 cable is connected to a current probe to measure the power noise 10 cm above the measured board, as shown in Fig. 20(a).

Figures 20(b) and 20(c) compare the measured $|S_{21}|$, which is used to determine the power noise in the power trace that passes through the reference board, which is used to determine the power noise in the trace that passes through the proposed filter structure for $f_r = 2.4$ GHz and $f_r = 5$ GHz, respectively. Figs. 20(b) and 20(c) show the substantial suppression of power noise by the proposed filter structure at around 1 GHz to 3.2 GHz and 6.5 GHz to 10 GHz for $f_r = 2.4$ GHz and 3.2 GHz to 4.5 GHz for $f_r = 5$ GHz, respectively. Despite the slight discrepancies, both the simulated results and actual measurements confirm the feasibility and usefulness of the reduction of noise by the proposed filter structure. Furthermore, the first resonant frequency is not the only reduction frequency: the 3rd resonant frequency is also a reduction frequency for $f_r = 2.4$ GHz case. Additionally, according to Fig. 18, the resonant frequencies of the cavity are evident in the $|S_{21}|$ values of the proposed filter structure without four additional ground vias. According to Fig. 19, the additional ground vias of the proposed filter structure significantly reduce the coupled noise (GBN).

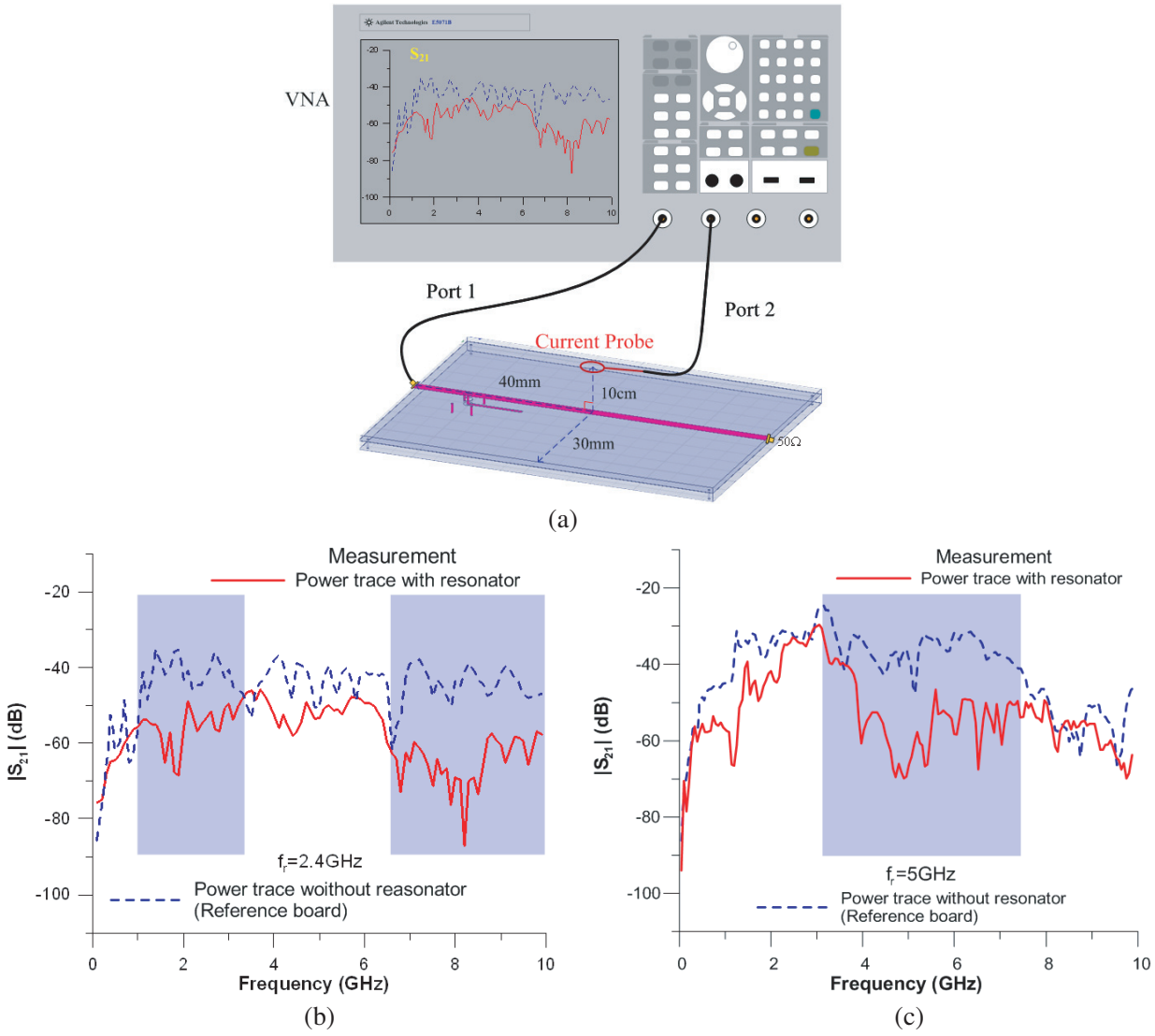

Figure 20. (a) Setup for measurement using vector network analyzer and current probe. (b) (c) Comparisons of simulated and measured $|S_{21}|$ values of proposed filter structure and reference board.

6. CONCLUSIONS

This work proposes a radio-frequency interference (RFI) noise suppression filter that generates little noise for a power trace. In the filter, a quarter-wavelength openstub resonator (QWOSR) is added to a multilayered high-speed digital PCB). RFI noise frequencies of 2.4 GHz and 5 GHz are considered in this work. The proposed filter structure is a four-layer multilayered PCB. The noise is reduced by the stripline trace of the QWOSR, the four additional ground vias adjacent to the QWOSR via, and shortening the via of the QWOSR. The noise, which includes peak noise of insertion loss ($|S_{21}|$), plane cavity resonance, ground bounce noise, and EM radiation noise, is reduced using the proposed RFI noise suppression filter. Shortening the via of the QWOSR reduces the generation of GBN. The stripline trace of the QWOSR between two ground planes can reduce the EM radiation noise. The four additional ground vias next to the QWOSR via significantly reduces the cavity resonance and GBN. The proposed filter structure must include four additional ground vias adjacent to the QWOSR via.

The electric field distributions verify that the insertion loss ($|S_{21}|$) values of the proposed filter structure with some peak responses result from the cavity resonance of the parallel ground planes. Time-domain ground bounce and power noise whose frequency is the same as or close to the resonant frequency of the QWOSR can be significantly reduced using the proposed filter structure. Finally, the favorable comparisons between the simulated and measured results and among the various measured results confirm the excellent noise reduction performance of the proposed filter structure.

ACKNOWLEDGMENT

The authors would like to thank NTUEE EDAPS Lab and Ansys Taiwan for providing measurement equipment and simulation software. They would also like to thank C. F. Huang for providing helpful information.

REFERENCES

1. https://www.wi-fi.org/.
2. Wu, T.-L., H.-H. Chuang, and T.-K. Wang, "Overview of power integrity solutions on package and PCB: Decoupling and EBG isolation," *IEEE Trans. Electromagn. Compat.*, Vol. 52, No. 2, 346–356, May 2010.
3. Hong, J.-S. G. and M. J. Lancaster, *Microstrip Filter for RF/Microwave Applications*, Ch. 6, Wiley, New York, NY, USA, 2001.
4. Leong, L.-I. A., C.-H. Tsai, and T.-L. Wu, "An ultra compact common-mode filter for RF Interference control in 3G wireless communication systems," *Proc. 2010 IEEE EMC Symposium*, 776–779, Aug. 1998.
5. Kim, B. and D.-W. Kim, "Improvement of simultaneous switching noise suppression of power plane using localized spiral-shaped EBG structure and lambda/4 open stubs," *Proc. Asia-Pacific Microw. Conf.*, 1–4, Dec. 2007.
6. Kasahara, Y., H. Toyao, and T. Harada, "Open stub electromagnetic bandgap structure for 2.4/5.2 GHz dual-band suppression of power plane noise," *Proc. IEEE Electr. Des. Adv. Packag. Syst. Symp.*, 1–4, Dec. 2011.
7. Shiue, G.-H., C.-M. Hsu, C.-L. Yeh, and C.-F. Hsu, "A comprehensive investigation of a common-mode filter for gigahertz differential signals using quarter-wavelength resonators," *IEEE Compon. Packag. Manuf. Technol.*, Vol. 4, No. 1, 134–144, Jun. 2014.
8. Hong, J.-S. G. and M. J. Lancaster, *Microstrip Filter for RF/Microwave Applications*, Ch. 6, Wiley, New York, NY, USA, 2001.
9. Lim, W. G., W. K. Kim, D. H. Shin, and J. W. Yu, "A novel bandstop filter design using parallel coupled line resonators," *Proc. 2007 European Microwave Conference*, 878–881, Oct. 2007.
10. Ege Engin, A. and J. Bowman, "Virtual ground fence for GHz power filtering on printed circuit boards," *IEEE Trans. Electromagn. Compat.*, Vol. 55, No. 6, 1277–1283, Nov. 2013.

11. Hao, Z. C., J. S. Hong, J. P. Parry, and D. P. Hand, "Ultra-wideband bandpass filter with multiple notch bands using nonuniform periodical slotted ground structure," *IEEE Trans. Microw. Theory Tech.*, Vol. 57, No. 12, 3080–3088, Dec. 2009.
12. Ansys, *Ansys HFSS. Ver. 13*, Pittsburgh, PA, USA [Online], Available: http://www.ansys.com, 2012.
13. Swaminathan, M. and A. E. Engin, *Power Integrity Modeling and Design for Semiconductors and Systems*, Prentice-Hall, Boston, MA, USA, 2007.
14. Kushta, T., K. Narita, T. Kaneko, T. Saeki, and H. Tohya, "Resonance stub effect in a transition from a through via hole to a stripline in multilayer PCBs," *IEEE Microw. Wireless Compon. Lett.*, Vol. 13, No. 5, 169–171, May 2003.
15. Deng, S., et al., "Effects of open stubs associated with plated through-hole vias in backpanel designs," *Proc. Int. Symp. Electromagn. Compat.*, 1017–1022, Aug. 2004.
16. Hall, S. H. and H. L. Heck, *Advanced Signal Integrity for High-Speed Digital System Design*, Ch. 10, Wiley, New York, NY, USA, 2009.
17. Lameres, B. J. and T. S. Kalkur, "The effect of ground vias on changing signal layers in a multilayered PCB," *Microwave and Optical Technology Letters*, Vol. 28, No. 4, 257–260, Feb. 2001.
18. Hwang, J. N. and T. L. Wu, "Coupling of the ground bounce noise to the signal trace with via transition in partitioned power bus of PCB," *Proc. IEEE Int. Symp. EMC*, 733–736, Minneapolis, MN, USA, Aug. 2006.
19. Guo, W. D., G. H. Shiue, C. M. Lin, and R. B. Wu, "An integrated signal and power integrity analysis for signal traces through the parallel planes using hybrid finite-element and finite-difference time-domain techniques," *IEEE Trans. Adv. Packag.*, Vol. 30, No. 3, 558–565, Aug. 2013.
20. Wu, C. T., G. H. Shiue, S. M. Lin, and R. B. Wu, "Composite effects of reflections and ground bounce for signal line through a split power plane," *IEEE Trans. Adv. Packag.*, Vol. 25, 297–301, May 2002.